RESEARCH ARTICLE

Characterizing aboveground biomass and tree cover of regrowing forests in Brazil using multi-source remote sensing data

Na Chen[1] (iD), Nandin-Erdene Tsendbazar[1], Daniela Requena Suarez[1], Jan Verbesselt[1] & Martin Herold[1,2]

[1]Laboratory of Geo-information Science and Remote Sensing, Wageningen University & Research, 6708 PB, Wageningen, Droevendaalsesteeg 3, The Netherlands
[2]Helmholtz GFZ German Research Centre for Geosciences, Section 1.4 Remote Sensing and Geoinformatics, 14473, Potsdam, Telegrafenberg, Germany

Abstract

Characterization of regrowing forests is vital for understanding forest dynamics to assess the impacts on carbon stocks and to support sustainable forest management. Although remote sensing is a key tool for understanding and monitoring forest dynamics, the use of exclusively remotely sensed data to explore the effects of different variables on regrowing forests across all biomes in Brazil has rarely been investigated. Here, we analyzed how environmental and human factors affect regrowing forests. Based on Brazil's secondary forest age map, 3060 locations disturbed between 1984 and 2018 were sampled, interpreted and analyzed in different biomes. We interpreted the time since disturbance for the sampled pixels in Google Earth Engine. Elevation, slope, climatic water deficit (CWD), the total Nitrogen of soil, cation exchange capacity (CEC) of soil, surrounding tree cover, distance to roads, distance to settlements and fire frequency were analyzed in their importance for predicting aboveground biomass (AGB) and tree cover derived from global forest aboveground biomass map and tree cover map, respectively. Results show that time since disturbance interpreted from satellite time series is the most important predictor for characterizing AGB and tree cover of regrowing forests. AGB increased with increasing time since disturbance, surrounding tree cover, soil total N, slope, distance to roads, distance to settlements and decreased with larger fire frequency, CWD and CEC of soil. Tree cover increased with larger time since disturbance, soil total N, surrounding tree cover, distance to roads, distance to settlements, slope and decreased with increasing elevation and CWD. These results emphasize the importance of remotely sensing products as key opportunities to improve the characterization of forest regrowth and to reduce data gaps and uncertainties related to forest carbon sink estimation. Our results provide a better understanding of regional forest dynamics, toward developing and assessing effective forest-related restoration and climatic mitigation strategies.

Introduction

Forests cover about 30% of the earth's land and provide various services to human society and store *approximately* 45% of terrestrial carbon (Bonan, 2008; Rodríguez-veiga et al., 2017; Valdés et al., 2020). While forest disturbances affect the delivery of forest ecosystem services, regrowing forests play important roles in global carbon sink dynamics (Pugh et al., 2019; Silva Junior et al., 2020). Regrowing forests here are defined as forests growing in areas where nearly complete removal of forest cover occurred. These forests are receiving growing attention as they usually have higher accumulation rates of aboveground biomass (AGB) compared with old-regrowth forests

(Oberleitner et al., 2021), and the 'regrowth capacity of the forest' is an indicator of the resilience of forests that is threatened by a mixture of human and climate stressors (e.g. logging, droughts and fires). Characterizing regrowing forests is essential for understanding forest dynamics and is beneficial for developing forest management strategies.

The spatial variability of AGB and tree cover of regrowing forests is affected by environmental conditions and degrees of human use. Understanding what drivers promote or hamper forest regrowth is essential for successful ecosystem restoration initiatives (César et al., 2021). However, the factors that influence regrowing forests vary by spatial scale (Becknell et al., 2018). Time is an essential driver of AGB and tree cover in regrowing forests and has been widely used because time is vital for successional processes (Becknell et al., 2018; Martin et al., 2013; Pugh et al., 2019). A previous study has even estimated age using AGB in Neotropical forests (Chazdon et al., 2016). Topography also plays an essential role in regrowing forests as the topography is related to temperature or other abiotic factors (Sundqvist et al., 2013); for example, biomass in regrowing forests tends to be larger at higher elevations in tropical dry forests (Salinas-Melgoza et al., 2018). Additionally, soil fertility affects tree growth and survival (César et al., 2021). Variations in soil have been shown to influence regrowing forests (e.g. AGB and species richness) at many sites (Oberleitner et al., 2021; Waring et al., 2015), for instance, the cation exchange capacity (CEC) of soil has been positively related to relative biomass recovery in the Neotropics (Poorter et al., 2016). Besides, the surrounding forest cover influences the seed composition and abundance (César et al., 2021; Crk et al., 2009) and AGB in regrowing forests has been shown to increase with surrounding tree cover in a tropical dry forests landscape (Requena Suarez et al., 2021). Climatic water deficit (CWD) has also been widely examined in regrowing forests (Chazdon et al., 2016; Heinrich et al., 2021; Poorter et al., 2016). For example, literature suggests that higher AGB is expected in areas of high water availability. Forest fire influences the biomass of forests, and it is a significant determinant for balancing forest carbon in tropical forests (Martins et al., 2012). Finally, degrees of human use, which can be evaluated through factors such as closeness to roads and settlements, are also critical for regrowing forests (Salinas-Melgoza et al., 2018). For instance, previous research has shown that distance to roads was positively related to regrowing forests (Crk et al., 2009). Examining different factors' effects on regrowing forests is beneficial for understanding how regrowing forests respond to different factors and provides information for improving the estimation of biomass and tree cover.

Numerous approaches (e.g. biome average, ground-based measurements and remote sensing approaches) can be used to characterize regrowing forests in terms of AGB or tree cover. The biome average method, which consists of estimating a single representative value of forest carbon for biomes, provides an important starting point but it is very difficult to assess the uncertainty of source data (Gibbs et al., 2007). Using ground data can improve the quantification of AGB in regrowing forests, but it is labor-intensive. On the contrary, remote sensing data and products can provide spatially and temporally intensive information for forest monitoring, especially in regions with low accessibility and limited ground data. For instance, in tropical and subtropical forests, because ecosystems are complex and the national forest monitoring capacities have limitations, most tropical countries still report carbon pools at 'Tier 1' level (default method of the 2006 IPCC) (Romijn et al., 2015). Remote sensing approaches have the potential to refine the estimates of forest carbon stocks (Gibbs et al., 2007). Recent studies synthesize available field data and remote sensing data to characterize forest carbon pools at a global scale (Cook-Patton et al., 2020; Harris et al., 2021; Requena Suarez et al., 2019). However, remote sensing products could be further utilized to reduce uncertainties and fill regional data gaps.

Remote sensing products offer further opportunities for studying the effects of different factors on regrowing forests in space and time. With the launch of the Landsat program, satellite images have been collected for more than 40 years (Wulder et al., 2019). Previous studies have used Landsat imagery to monitor the spectral recovery of regrowing forests directly (De Keersmaecker et al., 2022; Hermosilla et al., 2019; Hislop et al., 2018). With the assistance of satellite images, mapping forest age, tree cover and forest AGB at a regional or global level has become feasible (Santoro et al., 2021; Sexton et al., 2013; Silva Junior et al., 2020).

Investigating the effects of different factors on regrowing forests in Brazil is essential for reducing uncertainties related to forest carbon sink estimation; these effects are dynamic in space and time, and new or improved remote sensing products provide a great opportunity for studying them. Previous studies in regrowing forests have examined the relationship between AGB and drivers in the Amazon biome in Brazil (Heinrich et al., 2021) or the Neotropical region (Poorter et al., 2016). However, the relationship between regrowing forests and different factors using exclusively remote sensing data has not been investigated across all biomes of Brazil at a national level. This study focuses on evaluating the effects of different factors on regrowing forests in Brazil using exclusively remote sensing data and products. Here, we aim to

analyze how these factors affect regrowing forests (using aboveground biomass and tree cover as proxies) across all biomes of Brazil. For this purpose, we have selected the following factors: time since disturbance, elevation, slope, CWD, soil CEC, soil total Nitrogen, surrounding tree cover, fire frequency, distance to settlements and distance to roads. We further focused on factors that can be directly monitored using remote sensing data. Therefore, we investigated the influence of time since disturbance and surrounding tree cover to characterize AGB and tree cover in regrowing forests. Specifically, we aim to (1) analyze how the aforementioned spatial factors affect the biomass and tree cover of regrowing forests in Brazil, and (2) study the effect of 'time since disturbance' and 'surrounding tree cover' as remote sensing variables on AGB and tree cover in regrowing forest in particular. We selected the time since disturbance and surrounding tree cover for modelling because time is a significant driver of AGB (Anderson-Teixeira et al., 2016; Chazdon et al., 2007; Requena Suarez et al., 2019) and surrounding tree cover can be easily derived from earth observations with a reasonable spatial resolution (30 m) and temporal resolution.

Materials and Methods

Study area

Brazil covers more than 8.5 million km^2. Brazil is one of the most biodiverse countries on earth and encompasses six biomes, including the Amazon, Atlantic Forest, Caatinga, Cerrado, Pampa and Pantanal (Souza et al., 2020; Fig. 1). These six biomes cover distinct climatic and biological conditions. The Amazon biome is the largest biome (covering about 4.19 million km^2), which stores about 10% of the world's forest carbon (Heinrich et al., 2021). The Amazon biome also contains half of the world's rainforest (Roesch et al., 2009), and its regrowing forest accounts for about 20% of previously deforested land (Heinrich et al., 2021). The Atlantic Forest biome (c. 1.11 million km^2) stretches along the Brazilian coast and is one of the hottest and most diverse biodiversity hotspots on earth (Siminski et al., 2021). This biome mainly consists of tropical moist forests and tropical seasonal forests. The Caatinga biome (0.84 million km^2) consists of thorn shrubs and seasonally dry forests (Leal et al., 2005). The Cerrado (2.03 million km^2) is the second-largest Brazilian biome that is dominated by savanna formation (Zimbres et al., 2020). The Pampa biome covers an area of 0.17 million km^2 and its dominant vegetation is grasslands, sparse shrubs and tree formation (Roesch et al., 2009). Finally, the Pantanal biome encompasses an area of 0.17 million km^2 and comprises tropical wetlands, savanna and grassland (Souza et al., 2020).

Estimation of time since disturbance

Based on the secondary forest age map of Brazil (with a 30 m spatial resolution) derived from Land Use and Land Cover classification from Landsat images (Silva Junior et al., 2020), 3060 pixels were sampled in the six biomes of Brazil. To obtain a good quality of time since disturbance data, we visually interpreted the time since disturbance for the sampled pixels based on the normalized difference vegetation index (NDVI) time series trajectories and the true color composite of cloud-masked Landsat imagery from 1984 to 2019 in Google Earth Engine (GEE). Among these points, each biome consists of 510 points, and each time since disturbance (ranging from 1 to 34) consists of 15 points within each biome. We repeated the sample selection procedure until the criteria of 15 points for each time since disturbance within each biome was met.

Selected factors for regrowing forests

To test the effects of different factors on AGB and tree cover, we selected factors that provide spatially explicit data in the region and have been utilized in previous researches that mainly relied on ground data. Ten factors were used to analyze their effects on the AGB and tree cover of regrowing forests. To examine the effect of topography, elevation and slope were selected. The elevation (30 m spatial resolution) of the year 2000 was extracted from Shuttle Radar Topography Mission (Farr et al., 2007). Based on the elevation, the slope (in degrees) was calculated. CWD is the difference between monthly reference evapotranspiration and actual evapotranspiration (Abatzoglou et al., 2017). The CWD data (~4 km spatial resolution) were extracted from the 'Terra-Climate' dataset (Abatzoglou et al., 2017). Then, we selected all the monthly layers of CWD in the year 2019 and calculated the mean CWD. We extracted the soil total Nitrogen and the soil CEC from the 'Soil Grids 250m v2.0' product (De Sousa et al., 2020). The global soil dataset was used because SoilGrids 2.0 used the best available shared soil profile data from the world (De Sousa et al., 2020). Local soil datasets were unfortunately difficult to acquire. The mean values of soil total N and mean Soil CEC at 0–5 cm, 5–15 cm and 15–30 cm depths from De Sousa et al. (2020) were calculated. To evaluate the effect of surrounding forests, we calculated surrounding tree cover (ha). 500 m buffers were created for each sampling point, and then, the area of stable forests within the buffer zone of every point was calculated. To evaluate the effect of fire, fire frequency provided by the MapBiomas project (Mapbiomas Fire-Collection1; https://mapbiomas. org/en/colecoes-mapbiomas-1) was used to acquire the
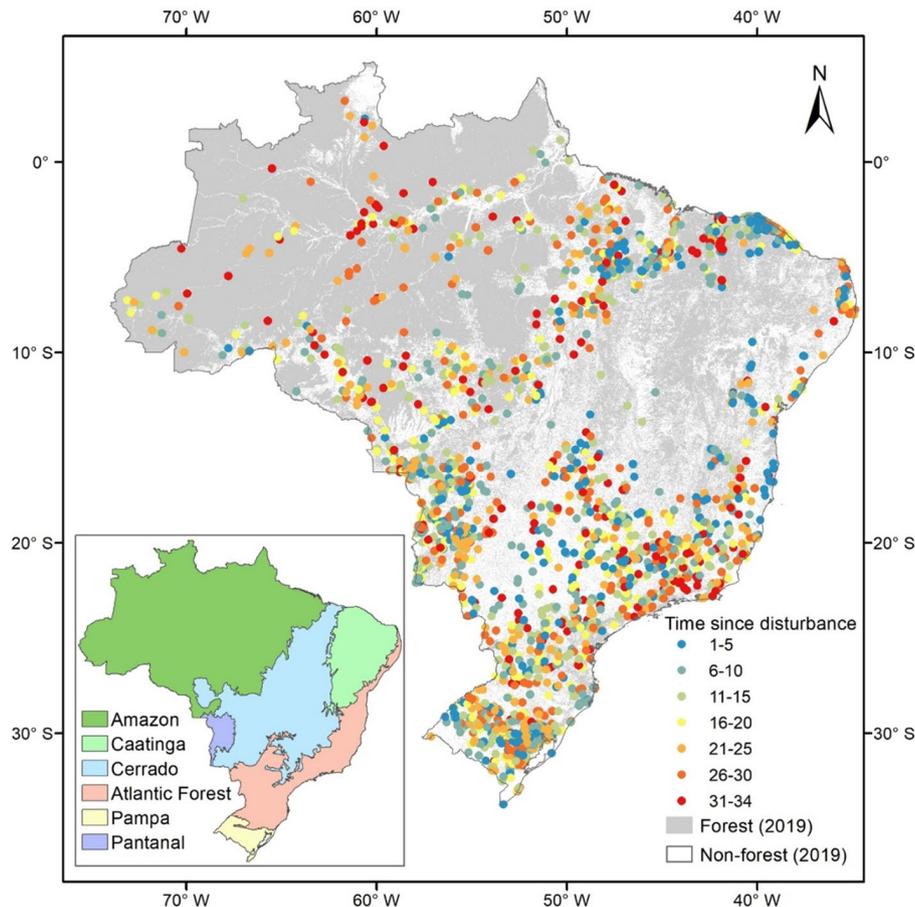
Figure 1. Study area and the distribution of sampled 3060 regrowth points across different time since disturbance groups in Brazil.

fire frequency from the year 1985 to 2019. To examine the effect of human use, we used distance to roads and settlements as proxies. Distances from sampling points to settlements and roads were obtained through the use of vector data from OpenStreetMap (OpenStreetMap Contributors 2021). Among all the selected factors, distance to settlements and roads were calculated using the 'Near' function of ArcMap 10.6.1. and the values of other factors of the sampled points were extracted in GEE. Table 1 shows the descriptive statistics of factors selected for characterizing regrowing forests.

Aboveground biomass and tree cover of regrowing forests

The values of aboveground biomass and tree cover were extracted to the sampled points in regrowing forests and stable forests, separately. Regrowing forest data include tree cover and AGB. The ESA Biomass Climate Change Initiative AGB map (100 m spatial resolution) (Santoro & Cartus, 2021) for the year 2018 was downloaded, clipped

by the boundary of Brazil and uploaded to Google Earth Engine (GEE). Tree cover data (30 m spatial resolution) can be accessed through Global Forest Cover Change products (Sexton et al., 2013), from which the 'tree_canopy_cover' layer was selected and the date was filtered by the year 2015. Then, the tree cover and AGB were extracted to the 3060 sampled points. Additionally, we also sampled another 3060 pixels (510 for each biome) within the extent of stable forests from the year 1985 to 2019 and extracted the AGB and tree cover values to those sampled points. To acquire the stable forest extent, land cover and land use (LUCC) maps were used from the MapBiomas Project (MapBiomas Collection 6; https://mapbiomas.org/en/colecoes-mapbiomas-1). Based on the LUCC maps (1985–2019), we first reclassified land cover and land use maps and assigned the forest pixels with value '0' and assigned '1' for other land cover types; then, we masked out the surface water in each year with the max water surface extent data provided by the Joint Research Centre (Pekel et al., 2016) to reduce commission errors of forest classification. Then, we overlayed all the

Table 1. Descriptive statistics of variables selected for characterizing regrowing forests.

Variable	Unit	Range	Mean	SD	Spatial resolution	Time	Source
AGB	Mg ha^{-1}	0–532.0	84.2	74.5	100 m	2018	Santoro et al. (2021)
Tree cover	%	0–84.0	34.3	19.4	30 m	2015	Sexton et al. (2013)
Time since disturbance	year	1–34.0	17.5	9.8	30 m	2019	Interpreted in this study
Elevation	meter	1–1797.0	297.2	293.1	30 m	2000	SRTM
Slope	degree	0–35.9	5.9	5.5	30 m	2000	Calculated
Climatic water deficit	mm/year	0–1256.7	350.9	210.8	4638 m	2019	UC Merced
Soil cation exchange capacity	mmol(c)/kg	0–285.0	133.6	44.9	250 m	/	De Sousa et al. (2021)
Soil total N (0–30 cm mean)	cg/kg	0–5562.0	1868.0	637.6	250 m	/	De Sousa et al. (2021)
Surrounding tree cover	ha	0–77.0	27.2	21.7	/	2019	Calculated from Mapbiomas
Distance to settlements	km	0–149.0	15.7	16.0	/	2021	OpenStreetMap contributors. (2021)
Distance to roads	km	0–88.8	1.9	4.9	/	2021	OpenStreetMap contributors. (2021)
Fire frequency (1985–2019)	times	0–14.0	0.5	1.3	30 m	1985–2019	Mapbiomas

forest layers from 1984 to 2019 to obtain the stable forest layer for this period.

Data analysis

To examine the effects of selected factors on AGB and tree cover in regrowing forests, we chose a mixed-effects modelling approach. This approach is suitable for highly structured data and accounts for fixed effects and random effects (Harrison et al., 2018). We applied mixed-effects models to analyze how different factors influence the AGB and tree cover of regrowing forests and study the effects of time since disturbance and the presence of nearby forests on regrowing forests. We fitted the models using:

$$y_{ij} = \beta_0 + \sum_{h=1}^{p}\beta_h x_{hij} + \alpha_j + \varepsilon_{ij} \tag{1}$$

$$\alpha_j \sim \text{Gaussian}\left(0, \sigma_\alpha^2\right) \tag{2}$$

$$\varepsilon_{ij} \sim \text{Gaussian}\left(0, \sigma_\varepsilon^2\right) \tag{3}$$

where y_{ij} is the value of the response variable for the jth groups, β_0 is the intercept, β_h represents the slope, x_{hij} is the ith value of the jth group for the hth predictor, α_j denotes random effects, ε_{ij} is the error for observation j, σ_α^2 and σ_ε^2 are within-group variances (Nakagawa & Schielzeth, 2013).

For all mixed-effects models, the Biome ID was specified as random effects to constrain the effect of random variability within biomes. For models using 10 selected variables, to avoid complex random structure and singular fit problems, the random slope was not specified, which means fitting models with fixed slopes and random

intercepts (Table 2). While, in the models that use only two variables, both time since disturbance and Biome ID are specified as random effects, meaning fitting models with random slopes and random intercepts. This indicates that the effect of time since disturbance on the response variables was assumed to vary between Biome IDs (Table 2).

Data have been transformed before modelling. To consider the non-linear increase in AGB and tree cover over time, we applied natural log transformation to the time since disturbance. Then, to make the effects comparable (Gelman & Hill, 2006), we scaled all the input variables by subtracting the average and dividing the difference by the standard deviations based on the 'scale' function in R. The variance inflation factor (VIF) (Marquardt, 1970) for all the explanatory variables was calculated, and all the VIFs were less than 5; thus, no variable was excluded for further analysis (Table S1). To fit the mixed-effects model, the package 'lme4' developed by Bates et al. (2015) was used. The model performance was assessed with marginal R^2 and conditional R^2 (Nakagawa & Schielzeth, 2013). The marginal R^2 is the proportion of variance explained by fixed factors, and the conditional R^2 is the proportion of variance explained by both fixed and random factors (Nakagawa & Schielzeth, 2013). The marginal R^2 and conditional R^2 were calculated by:

$$R_m^2 = \frac{\sigma_f^2}{\sigma_f^2 + \sum_{l=1}^{\mu}\sigma_l^2 + \sigma_e^2 + \sigma_d^2} \tag{4}$$

$$R_c^2 = \frac{\sigma_f^2 + \sum_{l=1}^{\mu}\sigma_l^2}{\sigma_f^2 + \sum_{l=1}^{\mu}\sigma_l^2 + \sigma_e^2 + \sigma_d^2} \tag{5}$$

where R_m^2 is the marginal R^2, R_c^2 is the conditional R^2, σ_f^2 represents the variance computed from the fixed effect components, σ_l^2 represents the variance component of the random factor, σ_e^2 denotes additive dispersion

Table 2. Overview of the specifications of fixed and random effects of each model.

Response variables	Fixed effects	Random effects
Ten selected variables		
AGB	Time since disturbance + Elevation + Slope + Climatic water deficit + Soil CEC + Soil total N + Surrounding tree cover + Distance to roads + Distance to settlements + Fire frequency	Biome ID (random intercepts)
Tree cover	Time since disturbance + Elevation + Slope + Climatic water deficit + Soil CEC + Soil total N + Surrounding tree cover + Distance to roads + Distance to settlements + Fire frequency	Biome ID (random intercepts)
Two selected variables		
AGB	Time since disturbance + Surrounding tree cover	Time since disturbance per Biome ID (random intercepts and slopes)
Tree cover	Time since disturbance + Surrounding tree cover	Time since disturbance per Biome ID (random intercepts and slopes)

components, and σ_d^2 is the distribution-specific variance (Nakagawa & Schielzeth, 2013).

Results

Characteristics of the sampled regrowing forests points

Across all biomes, AGB and tree cover increased with time since disturbance (as shown in Figs. 2 and 3). Additionally, the average biomass and tree cover of regrowing forests did not exceed those of stable forests.

Similarly, biome-specific average AGB and tree cover increased with time since disturbance despite fluctuations (as shown in Figs. 2 and 3). Additionally, the average AGB and tree cover of regrowing forests were less than those of stable forests. For the regrowing forest group with 31–34 years after disturbance, the mean AGB of the Amazon biome was the highest, followed by the Atlantic Forest, Cerrado, Pampa, Pantanal and Caatinga. For the same group, the mean tree cover (%) of the Amazon biome was the highest, followed by the Atlantic Forest, Cerrado, Pampa, Pantanal and Caatinga. Visually, the difference between the median values of AGB at 0–5 years and at 6–10 years after disturbances in the Caatinga biome was small. A similar trend can be found in tree cover in regrowing forests at 21–25, 26–30 and 31–34 years after disturbances in the Caatinga biome.

Effects of 10 selected factors on regrowing forests

Results from the first model showed that AGB increased with increasing time since disturbance, surrounding tree cover, soil total N, slope, distance to roads and distance to settlements (Fig. 4a). The effect of elevation was not

significant for modelling AGB in regrowing forests (Table S2). The model statistics (e.g. estimates, standard error, degrees of freedom, t-value and p-values) are shown in Table S2. AGB decreased with increasing fire frequency, CWD and CEC of soil. The marginal and conditional R^2 for the AGB model were 0.18 and 0.33, respectively. Based on the predicted AGB and tree cover from 1 to 34 years after disturbance, the biomass regrowing rate for the first 34 years was 2.98 Mg ha^{-1} year^{-1}.

Results from the second model showed that tree cover increased with increasing time since disturbance, soil total N, surrounding tree cover, distance to roads, distance to settlements and slope (Fig. 4b). The effects of soil CEC and fire frequency were not significant for modelling tree cover (Table S3). Tree cover decreased with increasing CWD and elevation. The marginal and conditional R^2 for the tree cover model were 0.22 and 0.33, respectively. The overall tree cover recovery rate during the first 34 years was 1.14% per year.

Effects of time since disturbance and surrounding tree cover on regrowing forests

We further focused on modelling AGB and tree cover on regrowing forests using time since disturbance and surrounding tree cover, which can be directly derived from earth observations with a reasonable spatial resolution (30 m) and temporal resolution. Results showed that both time since disturbance and surrounding tree cover had positive effects on AGB and tree cover (Fig. 5). AGB increased with increasing time since disturbance and surrounding tree cover (Fig. 5). Similarly, as the time since disturbance and surrounding tree cover increases, tree cover also increases (Fig. 5). Table 3 shows the various intercepts and coefficients for the mixed-effects models.
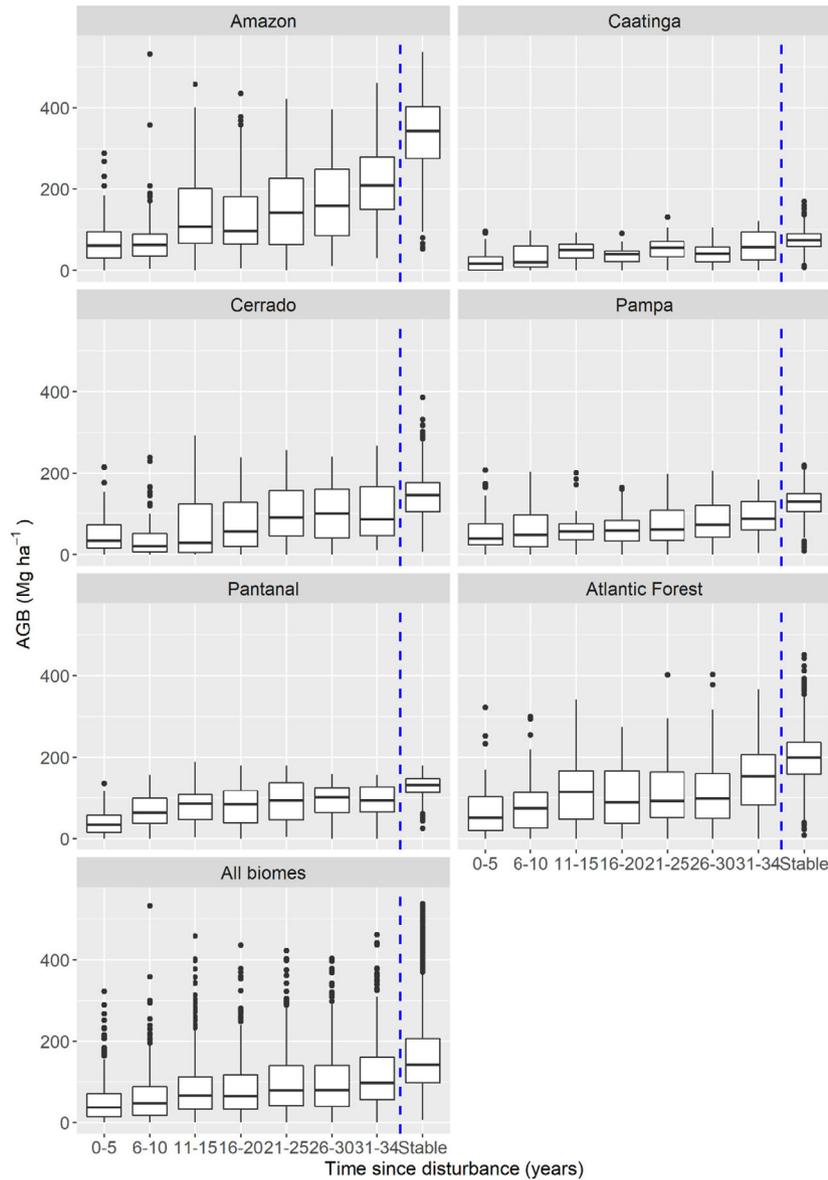
Figure 2. Distribution of AGB (in Mg ha^{-1}) in regrowing forests per category of time since disturbance (in years). The stable forest category is presented to the right of the dashed blue vertical line.

The model statistics are shown in Tables S4 and S5. For the AGB model, the slope coefficient of time since the disturbance in the Amazon biome was the largest, followed by the Atlantic Forest, Cerrado, Pantanal, Pampa and Caatinga. For the tree cover model, the slope coefficient of time since disturbance in the Amazon biome was the largest, followed by that of Atlantic Pantanal, Cerrado or Pampa, Atlantic Forest and Caatinga. The marginal R^2 for the AGB model was 0.11, and the conditional R^2 for the AGB model was 0.35. While the marginal R^2 for the tree cover model was 0.10, the conditional R^2 for the tree cover model was 0.34. The estimated AGB and tree cover

recovery rates during the first 34 years were 3.07 Mg ha^{-1} year^{-1} and 1.16% per year, respectively.

Discussion

We analyzed how selected factors (e.g. time since disturbance, CWD, fire frequency) affect the regrowing forests in Brazil. Variations in different predictors affect the AGB and tree cover of regrowing forests. We found that the assessed factors had varying effects on the AGB and tree cover of regrowing forests. AGB increased with increasing time since disturbance, surrounding tree cover, soil total
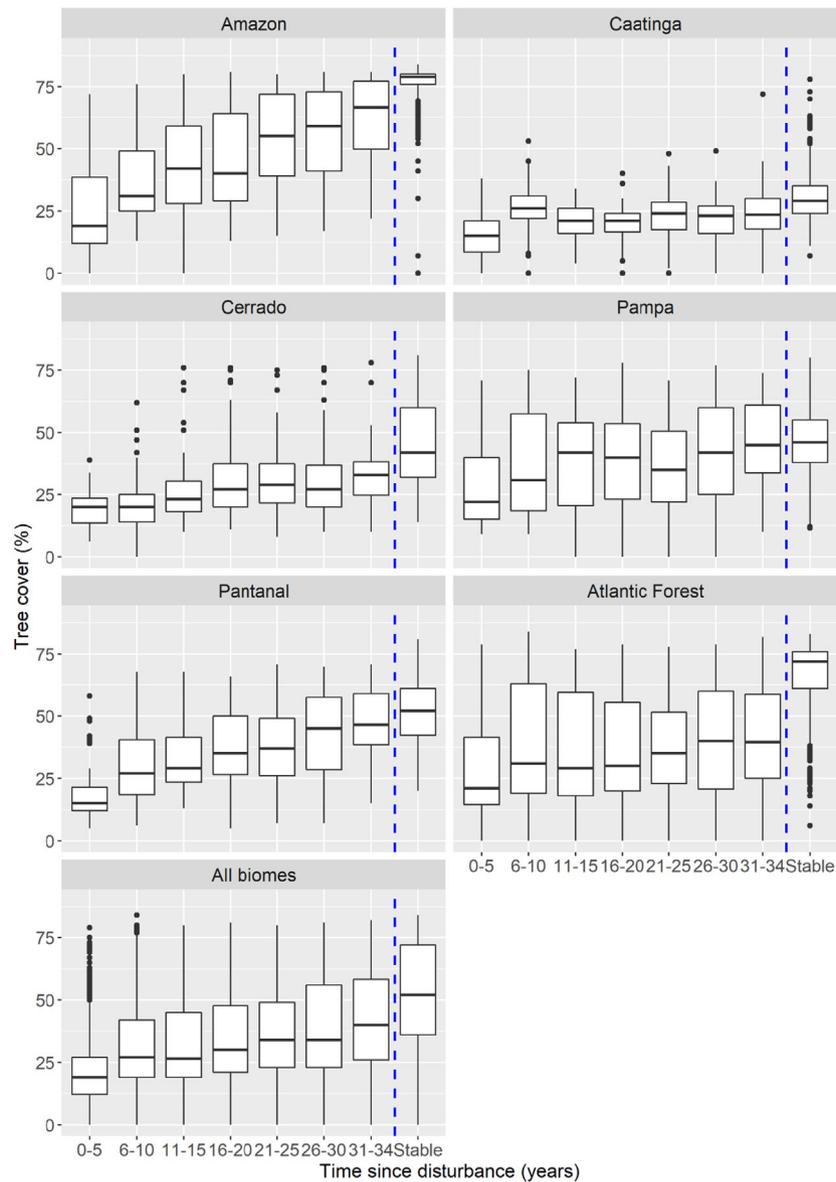
Figure 3. Distribution of tree cover (in %) in regrowing forests per category of time since disturbance (in years). The stable forest category is presented left of the dashed blue vertical line.

N, distance to roads and distance to settlements. It is logical to expect a positive effect of time since disturbance and surrounding tree cover on AGB recovery; our result aligns with the previous study on regrowing forests in the tropics that used field data (Poorter et al., 2016; Requena Suarez et al., 2021). The outliers for younger forests with time since disturbance from 0 to 5 in Figure 2. indicate that those young forests have extremely high biomass values, which could be explained by the mismatch between time since disturbance and AGB maps or errors in both. Soil nutrient content is known to influence forest AGB (Hofhansl et al., 2020; Lewis et al., 2013; Oberleitner

et al., 2021). Fertilization experiments were applied to evaluate the effects of Nitrogen and Phosphorus (P) on the AGB of secondary forest growth and results show that AGB increases significantly with N-only and N + P treatments (Davidson et al., 2004). Hence, our result of soil total Nitrogen's effect on AGB agrees with previous studies. As expected, AGB and tree cover increased with distance to settlements and distance to roads, a similar effect has been found in a previous study conducted in the Brazilian Atlantic Forest (Becknell et al., 2018). AGB decreased with larger fire frequency and increasing CWD. Forest fires can decrease biomass significantly in tropical
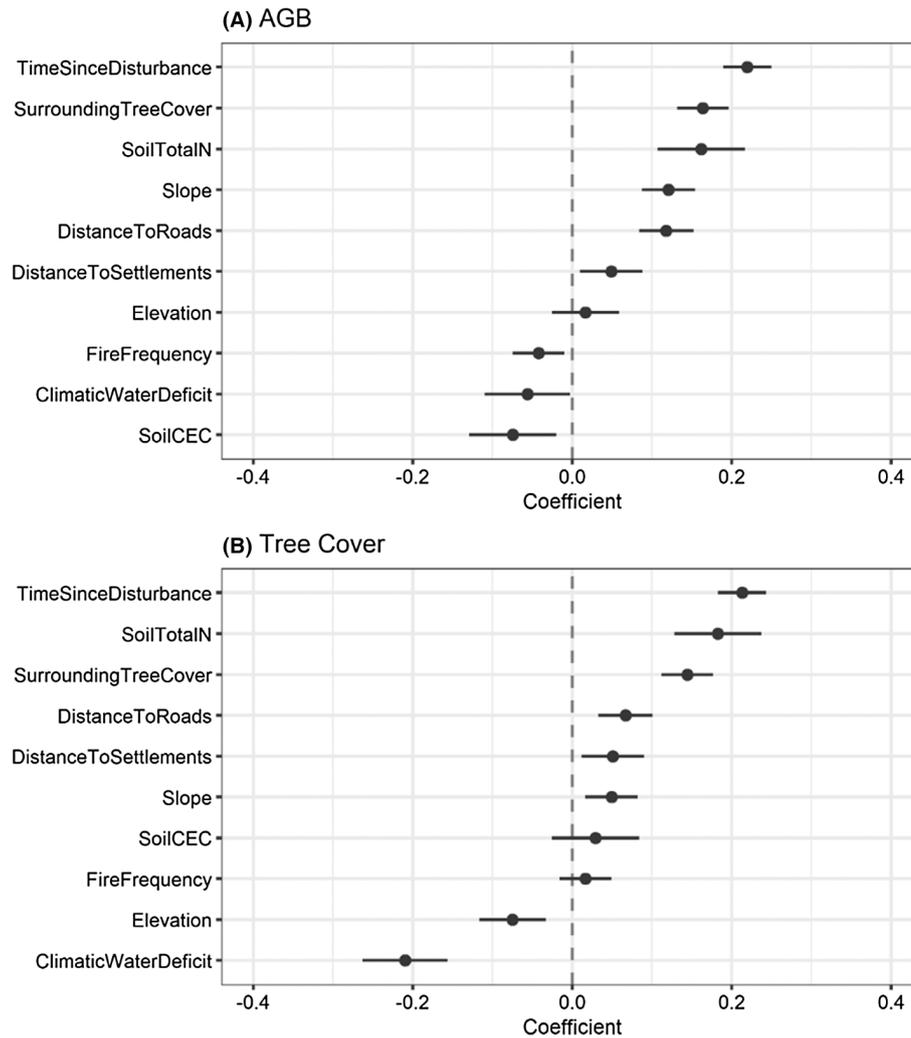
Figure 4. Effects of factors on (a) AGB (Mg ha^{-1}) and (b) Tree cover (%) of regrowing forests in Brazil. The vertical dashed line indicates no significant effect. The Dot-and-Whisker plots demonstrate the standardized coefficients and 95% confidence intervals for the mixed-effects model.

forests (Martins et al., 2012; Slik et al., 2008). AGB was shown to increase with decreasing CWD (Poorter et al., 2016). A previous study in the Neotropics has revealed a positive effect of CEC on relative AGB recovery (Poorter et al., 2016). Our results show that AGB decreases with increasing CEC of soil. Perhaps the effect of CEC on AGB recovery could be explained by the strong positive relationship between soil total N concentration and AGB or the CEC obtained from a global dataset and the small difference in soil may be overruled by the larger difference in microclimate (Poorter et al., 2016). It is hard to explain that slope is positively correlated with the AGB. Perhaps the areas with higher slopes could drain faster and have lower water tables (Daskin et al., 2019).

As expected, in order of decreasing importance, tree cover increased with time since disturbance, soil total N concentration, surrounding tree cover, distance to roads, distance to settlements and slope. Few recent studies have examined the influence of different factors on tree cover regrowth. It is logical that tree cover increased with increasing time since disturbance of regrowing forests because the surrounding tree cover affects seed availability and natural regeneration (César et al., 2021), and it was positively related to forest recovery (Jakovac et al., 2015; Requena Suarez et al., 2021). Soil nutrients affect forest growth; thus, it is reasonable that soil total N (as a proxy of soil nutrition) is positively related to tree cover. Tree cover increased with increasing distance to roads and settlements, suggesting that tree cover tends to recover faster
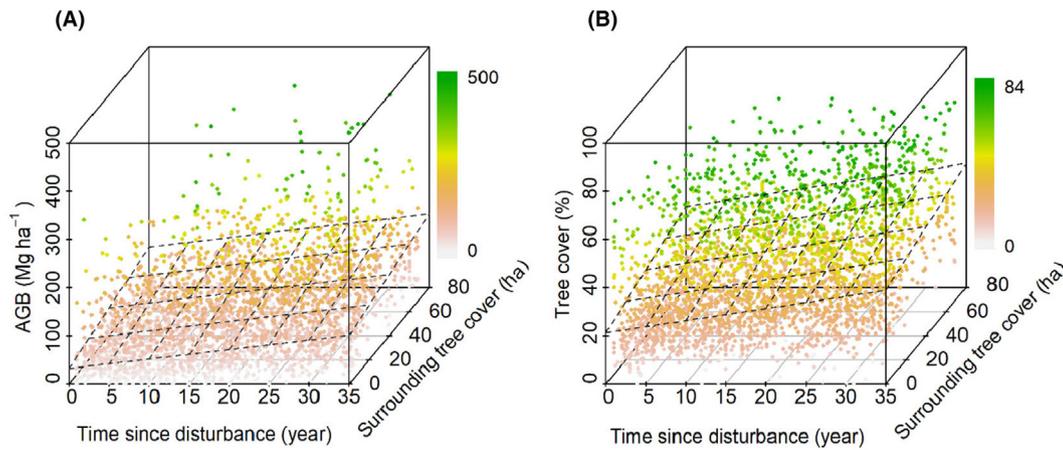
Figure 5. 3D scatter plots of all the 3060 sampled regrowing forest points and the regression planes of the fixed effects while modelling AGB and tree cover with time since disturbance and surrounding tree cover. (A) AGB (non-scaled data), (B) tree cover (non-scaled data). 3D scatter plots of 3060 sampled regrowing forest points and the regression planes of the fixed effects while modelling AGB and tree cover based on scaled data can be found in Figure S1.

Table 3. Coefficients of mixed-effects models for modelling AGB sand tree cover in Brazil using time since disturbance and surrounding tree cover.

	AGB			Tree cover		
	Intercept	Time since disturbance	Surrounding tree cover	Intercept	Time since disturbance	Surrounding tree cover
Fixed	<0.01	0.26	0.20	<0.01	0.26	0.18
Coefficients (Biome)						
Amazon	0.75	0.52	0.20	0.63	0.50	0.18
Caatinga	−0.66	0.11	0.20	−0.74	0.08	0.18
Cerrado	−0.05	0.25	0.20	−0.31	0.19	0.18
Pampa	−0.22	0.16	0.20	0.19	0.19	0.18
Pantanal	−0.17	0.21	0.20	−0.03	0.41	0.18
Atlantic forest	0.35	0.29	0.20	0.25	0.17	0.18

in less accessible regions. Previous studies have shown that frequent fires reduce tree cover in tropical floodplains (Daskin et al., 2019). Our results suggest that fire frequency was not significantly related to tree cover, which could be explained by the effect of fire on tree cover depending on climatic conditions (Staver et al., 2011) or perhaps the smaller difference in fire frequency may be overruled by the larger difference in climatic water deficit. Unexpectedly, the slope was positively related to tree cover, a previous study also revealed a similar relationship in the Brazilian Atlantic forest (Becknell et al., 2018). Water availability limits tree growth and tree cover increases with decreased CWD, which agrees with previous research that shows increased water deficit decreases tree growth (Restaino et al., 2016).

Our estimation of AGB recovery rates was smaller compared with global estimated rates conducted by Cook-Patton et al. (2020). To make results comparable, based on the global AGB accumulation rates map of the

first 30 years of regrowing forests developed by Cook-Patton et al. (2020), we clipped the global map to the boundary of Brazil and calculated the average regrowing forest rate of AGB change in Brazil for the first 30 years, which was 8.45 Mg ha^{-1} year^{-1}. To make our results comparable with the global map, we predicted the AGB accumulation rate at 30 years using the models with all selected variables, time since disturbance and surrounding tree cover models, and the predicted AGB rates are 3.30 and 3.38 Mg ha^{-1} year^{-1}, respectively (Table S6). Our estimated AGB change rates are lower than the aboveground carbon rates estimated by Cook-Patton et al. (2020), which integrated 13112 georeferenced field data of carbon accumulation and 66 environmental variables to model the carbon accumulation globally. To make our results comparable with previous studies, we also computed the AGB change rate for the first 20 years, the predicted recovery rate with all selected variables is 4.57 Mg ha^{-1} year^{-1} (Table S6). Similarly, our estimated

AGB accumulation rate is smaller compared with the biomass recovery rate in Neotropical secondary forests (6.1 Mg ha^{-1} year^{-1}) estimated by Poorter et al. (2016). The difference in estimating the recovery rates could be attributed to the different extents of the study areas and the use of only RS-derived data in our study. Regarding the biomass recovery rates in each biome, the extents of biomes in Brazil are different from the ecozones used in previous research conducted by Requena Suarez et al. (2019). Hence, we overlayed the ecozone map with the biome map and identified the main ecozone for each biome. The AGB recovery rate of the Amazon biome is 7.16 Mg ha^{-1}, which is higher than that of the tropical rainforest (5.9 Mg ha^{-1} year^{-1}) in the Americas (Requena Suarez et al., 2019). The AGB recovery rates of the Cerrado and Pantanal biomes are lower than that of tropical moist forests (5.2 Mg ha^{-1} year^{-1}) in the Americas (Requena Suarez et al., 2019). The AGB recovery rate of the Caatinga biome is lower than that of tropical dry forests (3.9 Mg ha^{-1} year^{-1}) in the Americas (Requena Suarez et al., 2019). Similarly, the difference in the AGB recovery rates could be attributed to the different study extents. Atlantic Forest was not compared as it mainly consists of three ecozones (tropical rainforest, tropical moist forest and subtropical moist forest). The Pampa biome is also not compared as it mainly overlays with the subtropical humid forest.

In this study, the determinants of AGB and tree cover in regrowing forests of Brazil were explored using exclusively remote sensing data and products. Our results not only show that remote sensing data and products are key resources for characterizing the AGB and tree cover of regrowing forests but also highlight the importance of using time since disturbance and surrounding tree cover, derived from remote sensing data, for characterizing regrowing forests. Future research could also explore the potential of using only time since disturbance for modelling AGB and surrounding tree cover in secondary forests as time since disturbance is a significant predictor, and it can be directly derived from the time series satellite images based on change detection algorithms. Our analysis provides a starting point for using exclusively remote sensing products to characterize regrowing forests, which could benefit the characterization of regrowing forests in regions where forest inventory data are scarce or not available. Further benefits also include regular monitoring of biomass in regrowing forests with high spatial and temporal resolution remote sensing data. Our analysis of different factors' impact on regrowing forests provides important information on what factors are useful for modelling AGB and tree cover of regrowing forests in Brazil, which is important for understanding regrowing forests dynamics as well as providing baseline information

for estimating carbon sinks and understanding the spatial variations of regrowing forests in Brazil. Understanding the carbon sinks in this region could benefit policymakers in evaluating the progress of reforesting 12 Mha of land proposed by the NDC of Brazil ('REDD+ and Brazil's NDC', 2019), thus providing critical information for climate mitigation initiatives. In addition, quantifying the regrowth rates of AGB and tree cover could provide a better understanding of the AGB and tree cover resilience and support policymakers for forest management and restoration plans.

Integrating field data or airborne laser scanning data into our analysis could potentially improve our modelling of aboveground biomass and tree cover of regrowing forests. For example, a previous study combined the field data and ALS data to estimate the AGB in a tropical landscape of Thailand (Jha et al., 2020). The integration of field data (e.g. aboveground biomass, time since disturbance) may potentially improve the performance of the models thus refining these initial results. Despite that using remote sensing data and products has disadvantages (e.g. indirect measurement of AGB, the occurrence of cloud and shadow in optical imagery), our analysis provides a starting point for understanding how different factors affect the AGB and tree cover of regrowing forests at a country scale. This provides important information for regions with low accessibility or scarce forest inventory, or field data that have a low temporal resolution. Besides, different remote sensing products not acquired in the same year introduce uncertainty, especially for the tree cover map, which is not available for the year 2019. Additionally, the different spatial resolutions of the remote sensing products may affect the accuracy of modelling regrowing forests. Future research could use data with less discrepancy in terms of spatial resolution or apply resample approach to reduce the mismatch between different remote sensing products. As the Landsat-based time since disturbance factor is a significant predictor (with a spatial resolution of 30 m) for regrowing forests, following studies could sample the regrowing forest patches that have an area larger than 1 ha ($\geq$1 pixel of the CCI biomass map). Next, the input data sources of the predictors should be considered as potential sources of circularity. Tree cover and time since disturbance were derived from Landsat imagery. To reduce the risk of circularity, a biomass map mainly derived from Sentinel-1 Envisat's ASAR instrument and ALOS was chosen. However, the SoilGrids 2.0 data used more than 400 environmental covariates, including raw bands and vegetation indices derived from Landsat imagery (De Sousa et al., 2020). Products derived from the same sensor suffer from the same artifacts. In addition, factor such as soil total N is sometimes modelled in function to vegetational succession. For example,

soil total N is expected to increase during forest succession (Duan et al., 2020), and the prediction of soil total N used the environmental covariates that include the vegetation status. This modelling could make the association between regrowing forests and soil total N circular and might cause inflation in the accuracy. Future studies could investigate the potential of using other soil products to reduce the circularity risk. Furthermore, scaling up our analysis from country scale to larger scales requires reliable information on time since disturbance or forest age, while the visual interpretation of time since disturbance is time-consuming. Further research could investigate the potential of using a global forest age map (Besnard et al., 2021). To ensure the quality of the forest age map, visual interpretation of satellite images could be useful for improving the map's accuracy. Finally, many other known factors influence regrowing forests. For example, the abundance of remnant forests (Zahawi et al., 2013), average annual shortwave (SW) radiation and the number of deforestations (Heinrich et al., 2021) have been observed to be significant for regrowing forests. While we attempted to examine the effects of several selected factors on regrowing forests, future research could integrate additional variables to refine the performance of models. Also, model selection approaches such as forward and backward stepwise selection could be applied to determine whether a variable should be included or removed for modelling AGB and tree cover.

Conclusions

Our study has assessed the effects of selected factors on regrowing forests in Brazil, finding that time since disturbance is a significant predictor for characterizing AGB and tree cover of regrowing forests in Brazil. We also used the time since disturbance and surrounding tree cover to model AGB and tree cover of regrowing forests. The recovery rates of AGB and tree cover in regrowing forests vary across different biomes. In addition, the AGB of regrowing forest is mainly affected by time since disturbance, surrounding tree cover, etc. and tree cover of regrowing forest is mainly affected by time since disturbance and climatic water deficit, etc. These factors can be extracted from remotely sensed data, and as such, our results emphasize the potential of using earth observation to characterize and monitor the AGB and tree cover of regrowing forests. Our analysis not only provides baseline information for understanding how these factors influence the AGB and tree cover but also reveals the climate mitigation potential of regrowing forest at the country scale since understanding the relative importance of different factors on regrowing forest provides information for estimating the carbon stocks. Additionally, the

observed effects of distance to roads and distance to settlements on the recovery of AGB and tree cover provide important information for future forest restoration initiatives.

References

Abatzoglou, J.T., Dobrowski, S.Z., Parks, S.A. & Hegewisch, K.C. (2017) Data descriptor: TerraClimate, a high-resolution global dataset of monthly climate and climatic water balance from 1958–2015. *Scientific Data*, **5**, 170191. https://doi.org/10.1038/sdata.2017.191

Anderson-Teixeira, K.J., Wang, M.M.H., McGarvey, J.C. & LeBauer, D.S. (2016) Carbon dynamics of mature and regrowth tropical forests derived from a pantropical database (TropForC-db). *Global Change Biology*, **22**(5), 1690–1709. https://doi.org/10.1111/gcb.13226

Bates, D., Mächler, M., Bolker, B.M. & Walker, S.C. (2015) Fitting linear mixed-effects models using lme4. *Journal of Statistical Software*, **67**(1), 1–48. https://doi.org/10.18637/jss.v067.i01

Becknell, J.M., Keller, M., Piotto, D., Longo, M., dos-Santos, M.N., Scaranello, M.A. et al. (2018) Landscape-scale lidar analysis of aboveground biomass distribution in secondary Brazilian Atlantic Forest. *Biotropica*, **50**(3), 520–530. https://doi.org/10.1111/btp.12538

Besnard, S., Koirala, S., Santoro, M., Weber, U., Nelson, J., Gütter, J. et al. (2021) Mapping global forest age from forest inventories, biomass and climate data. *Earth System Science Data*, **13**(10), 4881–4896. https://doi.org/10.5194/essd-13-4881-2021

Bonan, G.B. (2008) Forests and climate change: forcings, feedbacks, and the climate benefits of forests. *Science*, **320**, 1444–1449.

César, R.G., de Moreno, V.S., Coletta, G.D., Schweizer, D., Chazdon, R.L., Barlow, J. et al. (2021) It is not just about time: agricultural practices and surrounding forest cover affect secondary forest recovery in agricultural landscapes. *Biotropica*, **53**(2), 496–508. https://doi.org/10.1111/btp.12893

Chazdon, R.L., Broadbent, E.N., Rozendaal, D.M.A., Bongers, F., Zambrano, A.M.A., Aide, T.M. et al. (2016) Carbon sequestration potential of second-growth forest regeneration in the Latin American tropics. *Science Advances*, **2**(5), e1501639. https://doi.org/10.1126/sciadv.1501639

Chazdon, R.L., Letcher, S.G., van Breugel, M., Martínez-Ramos, M., Bongers, F. & Finegan, B. (2007) Rates of change in tree communities of secondary neotropical forests following major disturbances. *Philosophical Transactions of the Royal Society*, **362**(1478), 273–289. https://doi.org/10.1098/rstb.2006.1990

Cook-Patton, S.C., Leavitt, S.M., Gibbs, D., Harris, N.L., Lister, K., Anderson-Teixeira, K.J. et al. (2020) Mapping carbon accumulation potential from global natural forest regrowth. *Nature*, **585**(7826), 545–550. https://doi.org/10.1038/s41586-020-2686-x

Crk, T., Uriarte, M., Corsi, F. & Flynn, D. (2009) Forest recovery in a tropical landscape: what is the relative importance of biophysical, socioeconomic, and landscape variables? *Landscape Ecology*, **24**(5), 629–642. https://doi.org/10.1007/s10980-009-9338-8

Daskin, J.H., Aires, F. & Staver, A.C. (2019) Determinants of tree cover in tropical floodplains. *Proceedings of the Royal Society B: Biological Sciences*, **286**, 20191755. https://doi.org/10.1098/rspb.2019.1755

Davidson, E.A., Carvalho, C.J.R., Vieira, I.C.G., Figueiredo, R.O., Moutinho, P., Ishida, R.Y. et al. (2004) Nitrogen and phosphorus limitation of biomass growth in a tropical secondary forest. *Ecological Applications*, **14**(Suppl), 150–163. https://doi.org/10.1890/01-6006

De Keersmaecker, W., Rodríguez-Sánchez, P., Milencović, M., Herold, M., Reiche, J. & Verbesselt, J. (2022) Evaluating recovery metrics derived from optical time series over tropical forest ecosystems. *Remote Sensing of Environment*, **274**, 112991. https://doi.org/10.1016/j.rse.2022.112991

De Sousa, L.M., Poggio, L., Batjes, N.H., Heuvelink, G.B.M., Kempen, B., Ribeiro, E. et al. (2021) SoilGrids 2.0: producing quality-assessed soil information for the globe. *Soil Discuss*, **7**, 217–240. https://doi.org/10.5194/soil-7-217-2021

Duan, B., Man, X., Cai, T., Xiao, R. & Ge, Z. (2020) Increasing soil organic carbon and nitrogen stocks along with secondary forest succession in permafrost region of the Daxing'an mountains, Northeast China. *Global Ecology and Conservation*, **24**, e01258. https://doi.org/10.1016/j.gecco.2020.e01258

Farr, T.G., Rosen, P.A., Caro, E., Crippen, R., Duren, R., Hensley, S. et al. (2007) The shuttle radar topography mission. *Reviews of Geophysics*, **45**. https://doi.org/10.1029/2005RG000183

Gelman, A. & Hill, J. (2006) *Data analysis using regression and multilevel/hierarchical models*. Cambridge: Cambridge University Press. https://doi.org/10.1017/CBO9780511790942

Gibbs, H.K., Brown, S., Niles, J.O. & Foley, J.A. (2007) Monitoring and estimating tropical forest carbon stocks: making REDD a reality. *Environmental Research Letters*, **2**(4). https://doi.org/10.1088/1748-9326/2/4/045023

Harris, N.L., Gibbs, D.A., Baccini, A., Birdsey, R.A., de Bruin, S., Farina, M. et al. (2021) Global maps of twenty-first century forest carbon fluxes. *Nature Climate Change*, **11**, 234–240. https://doi.org/10.1038/s41558-020-00976-6

Harrison, X.A., Donaldson, L., Correa-Cano, M.E., Evans, J., Fisher, D.N., Goodwin, C.E.D. et al. (2018) A brief introduction to mixed effects modelling and multi-model inference in ecology. *PeerJ*, **6**, e4794. https://doi.org/10.7717/peerj.4794

Heinrich, V.H.A., Dalagnol, R., Cassol, H.L.G., Rosan, T.M., De Almeida, C.T., Junior, C.H.L.S. et al. (2021) Large carbon sink potential of secondary forests in the Brazilian Amazon to mitigate climate change. *Nature Communications*, **12**, 1785. https://doi.org/10.1038/s41467-021-22050-1

Hermosilla, T., Wulder, M.A., White, J.C. & Coops, N.C. (2019) Prevalence of multiple forest disturbances and impact on vegetation regrowth from interannual Landsat time series (1985–2015). *Remote Sensing of Environment*, **233**, 111403. https://doi.org/10.1016/j.rse.2019.111403

Hislop, S., Jones, S., Soto-Berelov, M., Skidmore, A., Haywood, A. & Nguyen, T.H. (2018) Using landsat spectral indices in time-series to assess wildfire disturbance and recovery. *Remote Sensing*, **10**(3), 460. https://doi.org/10.3390/rs10030460

Hofhansl, F., Chacón-madrigal, E., Fuchslueger, L., Jenking, D., Morera-beita, A., Plutzar, C. et al. (2020) Climatic and edaphic controls over tropical forest diversity and vegetation carbon storage. *Scientific Reports*, **10**, 5066. https://doi.org/10.1038/s41598-020-61868-5

Jakovac, C.C., Penã-Claros, M., Kuyper, T.W. & Bongers, F. (2015) Loss of secondary forest resilience by land-use intensification in the Amazon. *Journal of Ecology*, **103**, 67–77.

Jha, N., Kumar Tripathi, N., Chanthorn, W., Brockelman, W., Nathalang, A., Pelissier, R. et al. (2020) Forest aboveground biomass stock and resilience in a tropical landscape of Thailand. *Biogeosciences*, **17**(1), 121–134. https://doi.org/10.5194/bg-17-121-2020

Leal, I.R., Da Silva, J.M.C., Tabarelli, M. & Lacher, T.E. (2005) Changing the course of biodiversity conservation in the caatinga of northeastern Brazil. *Conservation Biology*, **19**(3), 701–706. https://doi.org/10.1111/j.1523-1739.2005.00703.x

Lewis, S.L., Bonaventure, S., Sunderland, T., Begne, S.K., Lopez-gonzalez, G., Van Der Heijden, G.M.F. et al. (2013) Aboveground biomass and structure of 260 African tropical forests. *Philosophical Transactions of the Royal Society, B Biological Sciences*, **368**(1625), 20120295. https://doi.org/10.1098/rstb.2012.0295

Marquardt, D.W. (1970) Generalized inverses, ridge regression, biased linear estimation, and nonlinear estimation. *Technometrics*, **12**, 591–612. https://doi.org/10.1080/00401706.1970.10488699

Martin, P.A., Newton, A.C. & Bullock, J.M. (2013) Carbon pools recover more quickly than plant biodiversity in tropical secondary forests. *Proceedings of the Royal Society B: Biological Science*, **280**(1773), 20132236. https://doi.org/10.1098/rspb.2013.2236

Martins, F.S.R.V., Xaud, H.A.M., dos Santos, J.R. & Galvão, L.S. (2012) Effects of fire on aboveground forest biomass in the northern Brazilian Amazon. *Journal of Tropical Ecology*, **28**(6), 591–601. https://doi.org/10.1017/S0266467412000636

Nakagawa, S. & Schielzeth, H. (2013) A general and simple method for obtaining R2 from generalized linear mixed-effects models. Methods Ecol. *Evol.* **4**, 133–142. https://doi.org/10.1111/j.2041-210x.2012.00261.x

Oberleitner, F., Egger, C., Oberdorfer, S., Dullinger, S., Wanek, W. & Hietz, P. (2021) Recovery of aboveground biomass, species richness and composition in tropical secondary forests in SW Costa Rica. *Forest Ecology and Management*, **479**, 118580. https://doi.org/10.1016/j.foreco.2020.118580

OpenStreetMap Contributors. (2021) OpenStreetMap. Available from: http://download.geofabrik.de/south-america/brazil.html [Accessed 4th June, 2021].

Pekel, J.F., Cottam, A., Gorelick, N. & Belward, A.S. (2016) High-resolution mapping of global surface water and its long-term changes. *Nature*, **540**, 418–422. https://doi.org/10.1038/nature20584

Poorter, L., Bongers, F., Aide, T.M., Almeyda Zambrano, A.M., Balvanera, P., Becknell, J.M. et al. (2016) Biomass resilience of neotropical secondary forests. *Nature*, **530**(7589), 211–214. https://doi.org/10.1038/nature16512

Pugh, T.A.M., Lindeskog, M., Smith, B., Poulter, B., Arneth, A. & Haverd, V. (2019) Role of forest regrowth in global carbon sink dynamics. *Proceedings of the National Academy of Sciences*, **116**(10), 4382–4387. https://doi.org/10.1073/pnas.1810512116

REDD+ and Brazil's Nationally Determined Contribution. (2019, October 4). Available from: http://redd.mma.gov.br/en/redd-and-brazil-s-ndc

Requena Suarez, D.R., Rozendaal, D.M.A., De Sy, V., Phillips, O.L., Alvarez-Dávila, E., Anderson-Teixeira, K. et al. (2019) Estimating aboveground net biomass change for tropical and subtropical forests: refinement of IPCC default rates using forest plot data. *Global Change Biology*, **25**(11), 3609–3624. https://doi.org/10.1111/gcb.14767

Requena Suarez, D., Rozendaal, D.M.A., De Sy, V. & Gibbs, D. (2021) Variation in aboveground biomass in forests and woodlands in Tanzania along gradients in environmental conditions and human use. *Environmental Research Letters*, **16**, 044014. https://doi.org/10.1088/1748-9326/abe960

Restaino, C.M., Peterson, D.L. & Littell, J. (2016) Increased water deficit decreases Douglas fir growth throughout western US forests. *Proceedings of the National Academy of Sciences*, **113**(34), 9557–9562. https://doi.org/10.1073/pnas.1602384113

Rodríguez-veiga, P., Wheeler, J., Louis, V., Tansey, K. & Balzter, H. (2017) Quantifying Forest biomass carbon stocks from space. *Current Forestry Reports*, **3**, 1–18. https://doi.org/10.1007/s40725-017-0052-5

Roesch, L.F.W., Vieira, F.C.B., Pereira, V.A., Schünemann, A.L., Teixeira, I.F., Senna, A.J.T. et al. (2009) The Brazilian Pampa: a fragile biome. *Diversity*, **1**(2), 182–198. https://doi.org/10.3390/d1020182

Romijn, E., Lantican, C.B., Herold, M., Lindquist, E., Ochieng, R., Wijaya, A. et al. (2015) Assessing change in national forest monitoring capacities of 99 tropical countries. *Forest Ecology and Management*, **352**, 109–123. https://doi.org/10.1016/j.foreco.2015.06.003

Salinas-Melgoza, M.A., Skutsch, M. & Lovett, J.C. (2018) Predicting aboveground forest biomass with topographic variables in human-impacted tropical dry forest landscapes. *Ecosphere*, **9**(1), e02063. https://doi.org/10.1002/ecs2.2063

Santoro, M. & Cartus, O. (2021) *ESA biomass climate change initiative (biomass_cci): global datasets of forest aboveground biomass for the years 2010, 2017 and 2018, v2.* Centre for Environmental Data Analysis. https://doi.org/10.5285/84403d09cef3485883158f4df2989b0c

Santoro, M., Cartus, O., Carvalhais, N., Rozendaal, D., Avitabilie, V., Araza, A. et al. (2021) The global forest aboveground biomass pool for 2010 estimated from high-resolution satellite observations. *Earth System Science Data*, **13**(8), 3927–3950. https://doi.org/10.5194/essd-2020-148

Sexton, J.O., Song, X.P., Feng, M., Noojipady, P., Anand, A., Huang, C. et al. (2013) Global, 30-m resolution continuous fields of tree cover: Landsat-based rescaling of MODIS vegetation continuous fields with lidar-based estimates of error. *International Journal of Digital Earth*, **6**(5), 427–448. https://doi.org/10.1080/17538947.2013.786146

Silva Junior, C.H.L., Heinrich, V.H.A., Freire, A.T.G., Broggio, I.S., Rosan, T.M., Do, J. et al. (2020) Benchmark maps of 33 years of secondary forest age for Brazil. *Scientific Data*, **7**(1), 269. https://doi.org/10.1038/s41597-020-00600-4

Siminski, A., Zambiazi, D.C., dos Santos, K.L. & Fantini, A.C. (2021) Dynamics of natural regeneration: implications for landscape restoration in the Atlantic Forest, Brazil. *Frontiers in Forests and Global Change*, **4**. https://doi.org/10.3389/ffgc.2021.576908

Slik, J.W.F., Bernard, C.S., Beek, M.V., Breman, F.C. & Eichhorn, K.A.O. (2008) Tree diversity, composition, forest structure and aboveground biomass dynamics after single and repeated fire in a Bornean rain forest. *Oecologia*, **158**(3), 579–588. https://doi.org/10.1007/s00442-008-1163-2

Souza, C.M., Jr., Schimbo, J.Z., Rosa, M.R., Parente, L.L., Alencar, A.A. & Rudorff, B.F. (2020) Reconstructing three decades of land use and land cover changes in brazilian

biomes with landsat archive and earth engine. *Remote Sensing*, **12**(17), 2735. https://doi.org/10.3390/RS12172735

Staver, A.C., Archibald, S. & Levin, S. (2011) Tree cover in sub-Saharan Africa: rainfall and fire constrain forest and savanna as alternative stable states. *Ecology*, **92**(5), 1063–1072. https://doi.org/10.1890/i0012-9658-92-5-1063

Sundqvist, M.K., Sanders, N.J. & Wardle, D.A. (2013) Community and ecosystem responses to elevational gradients: processes, mechanisms, and insights for global change. *Annual Review of Ecology, Evolution, and Systematics*, **44**, 261–280. https://doi.org/10.1146/annurev-ecolsys-110512-135750

Valdés, A., Lenoir, J., Frenne, P.D., Andrieu, E., Brunet, J., Chabrerie, O. et al. (2020) High ecosystem service delivery potential of small woodlands in agricultural landscapes. *Journal of Applied Ecology*, **57**, 4–16. https://doi.org/10.1111/1365-2664.13537

Waring, B.G., Becknell, J.M. & Powers, J.S. (2015) Nitrogen, phosphorus, and cation use efficiency in stands of regenerating tropical dry forest. *Oecologia*, **178**(3), 887–897. https://doi.org/10.1007/s00442-015-3283-9

Wulder, M.A., Loveland, T.R., Roy, D.P., Crawford, C.J., Masek, G., Woodcock, C.E. et al. (2019) Current status of Landsat program, science, and applications. *Remote Sensing of Environment*, **225**, 127–147. https://doi.org/10.1016/j.rse.2019.02.015

Zahawi, R.A., Holl, K.D., Cole, R.J. & Reid, J.L. (2013) Testing applied nucleation as a strategy to facilitate tropical forest recovery. *Journal of Applied Ecology*, **50**(1), 88–96. https://doi.org/10.1111/1365-2664.12014

Zimbres, B., Shimbo, J., Bustamante, M., Levick, S., Miranda, S., Roitman, I. et al. (2020) Savanna vegetation structure in the Brazilian Cerrado allows for the accurate estimation of aboveground biomass using terrestrial laser scanning. *Forest Ecology and Management*, **458**, 117798. https://doi.org/10.1016/j.foreco.2019.117798

Supporting Information

Additional supporting information may be found online in the Supporting Information section at the end of the article.

Data S1